actuators

MDPI

Article

An ARX Model-Based Predictive Control of a Semi-Active Vehicle Suspension to Improve Passenger Comfort and Road-Holding

Alejandro Piñón [1], Antonio Favela-Contreras [1,*], Luis C. Félix-Herrán [2], Francisco Beltran-Carbajal [3] and Camilo Lozoya [4]

1 School of Engineering and Sciences, Tecnologico de Monterrey, Ave. Eugenio Garza Sada 2501, Monterrey 64849, Mexico; a00802897@itesm.mx
2 School of Engineering and Sciences, Tecnologico de Monterrey, Blvd. Enrique Mazón López 965, Hermosillo 83000, Mexico; lcfelix@tec.mx
3 Departamento de Energía, Universidad Autónoma Metropolitana, Unidad Azcapotzalco, Av. San Pablo No. 180, Col. Reynosa Tamaulipas, Mexico City 02200, Mexico; fbeltran.git@gmail.com
4 School of Engineering and Science, Tecnologico de Monterrey, Av. H. Colegio Militar 4700, Nombre de Dios, Chihuahua 31300, Mexico; camilo.lozoya@tec.mx
* Correspondence: antonio.favela@tec.mx; Tel.: +52-8183-58-2000

Abstract: Passenger comfort and vehicle stability are key aspects that must be guaranteed on ground vehicles, and semi-active suspensions have offered an outstanding solution to meet these opposite objectives. This contribution describes a novel autoregressive with exogenous input (ARX) model-based predictive control strategy handled by a driver block applied on a semi-active vehicle suspension to improve passenger comfort and road holding when compared against a passive vehicle suspension system and another more complex control designs reported in the literature. The ARX model employs a driver block to reduce the computational load of the closed-loop semi-active suspension. In addition, the controller's formulation and the case study consider the actuator's physical constraints to achieve more realistic results. This case-study includes a one-quarter semi-active suspension with two degrees-of-freedom, and the numerical data comes from a real magnetorheological damper characterization. The results, in frequency-domain and time-domain, are measured based on specific performance criteria. A substantial improvement against a passive suspension is quantified and discussed. For a broader perspective of the findings, the results are compared against another reported work. This research effort could be the basis of further studies to achieve more robust solutions such as adaptive/optimal predictive controllers to improve vehicle's comfort and stability.

Keywords: predictive control; ARX model; vibration control; actuator's physical constraints; semi-active suspension

Citation: Piñón, A.; Favela-Contreras, A.; Félix-Herrán, L.C.; Beltran-Carbajal, F.; Lozoya, C. An ARX Model-Based Predictive Control of a Semi-Active Vehicle Suspension to Improve Passenger Comfort and Road-Holding. *Actuators* **2021**, *10*, 47. https://doi.org/10.3390/act10030047

Academic Editor: Kenji Uchino

Received: 18 January 2021
Accepted: 25 February 2021
Published: 2 March 2021

1. Introduction

Among other advantages, the suspension system of a ground vehicle contributes to the provision of passenger comfort and vehicle stability [1–3]. This impact on comfort and stability has driven great efforts and collaboration to improve both indexes at the same time, although passenger comfort and vehicle stability are opposite indicators [4]. Different suspension structures, materials, mathematical models, sensors, actuators, and control strategies have been reported in each of these lines of study, so the efforts to improve the suspension system are very extensive.

From the point of view of the force that a suspension can provide, there are three types of suspensions: passive, semi-active, and active. In the passive case, the suspension generates a force directly proportional to the difference between the speed of the suspended and unsprung masses; it can be said that there is a constant of proportionality established when

the shock absorber was designed, and this value cannot be changed during the damper´s life cycle. The semi-active option has a damper with a baseline value of force, which can be increased by applying an extra stimulus. With this characteristic, the restoring force can be varied in real-time. The active solution also changes the damper's characteristics during the operation, but there is no base value, so external energy must always be applied to the suspension or the force applied to the system will be totally lost [5]. Moreover, it has been proven that semi-active suspensions require fewer resources than an active one and they can also achieve the levels of force required to meet the comfort and stability indexes established in the performance tests [5,6].

Additionally, this type of suspension surpasses the passive one, which is unable to modify the damper´s characteristics during the system's operation. From the studied actuator options in semi-active solutions, some of the most studied are electro-rheological (ER) and magneto-rheological (MR) dampers [7]. MR dampers are most frequently applied because they have lower power consumption and better safety conditions than ER dampers [8–11]. With these arguments, this research focuses on the design of a control system for a semi-active suspension whose actuator is an MR damper.

One of the requirements about designing controllers for semi-active suspensions with MR dampers is to have a model that represents the system´s dynamics and that is suitable for control purposes. MR dampers are actuators with special rheologic properties that are represented with non-linear mathematical models that include saturation, hysteresis, and the flow of rheological fluids through an orifice [8]. The phenomenological model proposed by Bouc-Wen [12] has been widely used to describe MR dampers because it efficiently represents the damper's non-linearities and it can be applied for diverse control purposes [13–16], and this is the approach applied herein. To also limit the scope of the study, it has been decided to work with a two-degrees-of-freedom DOF suspension limited to vertical dynamics.

After the actuator's model have been selected, the challenge is to include the actuators dynamics in the controller's design to have a solution closer to reality. A reported option has been the insertion of the Bouc-Wen model in the system's identification process [17] for further control design [18]. The advantage of using this approach is that it includes the non-linear dynamics of the actuator, represented by the Bouc-Wen equations, in such a way that the manipulation signal, i.e., the force delivered by the MR damper, considers the actuator's dynamics and its limitations as well. These considerations contribute to generate findings closer to reality.

With the modelling issues addressed, the next step is to design the controller. The universe of control strategies reported for a 2-DOF one-quarter vehicle is diverse and includes a wide range of solutions, such as fuzzy controllers [19,20], $H\infty/H_2$ solutions [21–23], sliding mode controllers [24,25], Linear Parameter-Varying control [26,27], Linear Quadratic regulator (LQR) [28], active suspension control with online estimation [29], among others. Moreover, complementary techniques to a pure control strategy have been developed to improve suspension performance in changing scenarios [30–32].

Another research path in control of vehicle suspension includes the family of controllers based on predictive models. MPC (model predictive control) has been applied with different approaches. Neural-Network (NN)-MPC [33], Stochastic MPC [34], MPC with Preview Control [35,36], Distributed-MPC [37], Multiplexed-MPC with a Kalman filter [38], fast-MPC [39], Explicit-MPC [40], Hybrid MPC-Optimal [41], LPC-MPC-FaultTolerant [42], and also solutions that include Cloud-Computing [43]. Based on solutions reported in MPC, it is observed a considerable effort to comply with the performance criteria for vehicle suspensions.

Within the MPC family, there are practically no reported results of MPC based on ARX (autoregressive with exogenous input) models applied to vehicle suspensions, and this is part of the motivation to carry out this research. To the best of the authors' knowledge, there is very few reported work about MPC based on ARX models for vehicle suspensions. It is an adaptive MPC focused on controlling yaw dynamics for a four-tires suspension in

an electrically-actuated-vehicle. The reported control system is based on the ARX model of vehicle yaw dynamics [44]. The proposal is to develop a predictive approach based on the system's model, including the actuator's dynamics. For suspension performance it is very important to consider the actuator's limitations for control design, as recently reported in [45]. This research effort could be the basis of further studies with more robust solutions such as adaptive and/or optimal controllers for MPC based on ARX models.

The herein reported contribution is the design of a predictive controller based on an ARX model that avoids online optimizations, considers the actuator's physical restrictions, and is applied in a nonlinear mechanical system which represents a system of great interest to the automotive sector. The developed solution differs from traditional predictive control approaches in that it employs a driver block without the need of an online optimization algorithm reducing computational effort, and this simplifies the implementation of the control. Avoiding the execution of online optimization is perceived as part of the contribution of this work, from the perspective of saving computational resources. The controller design also includes an identification process of the system, which modeling takes account of the actuator's nonlinear dynamics.

The case study is an electro-mechanical 2-DOF system limited to vertical dynamics. Moreover, the applied criteria to evaluate the suspension´s efficiency come from ISO standards [2] and another specific qualitative and quantitative criteria employed to evaluate suspension performance [18,21].

The main objectives of this work are to improve the passenger's comfort and vehicle stability by means of a semi-active suspension with a predictive controller. The current research stage is the 2-DOF suspension system, limited to vertical dynamics, with the disadvantage of a having only vertical dynamics, but with the expectation of extending the study to 1/2 and full vehicle. The driver block in the proposed predictive controller that contains an ARX model is an innovative idea not found in suspension systems that could lead to promising findings.

The applied research methodology is as follows: a review of the state of the art was carried out and it was detected that a semi-active suspension with the predictive controller as developed here, had not been reported. With this finding and with the interest in finding different ways to improve passenger comfort and vehicle stability, the predictive controller strategy was designed and adapted to a semi-active one-quarter vehicle suspension with a MR damper. Based on the performance criteria (time-domain and frequency-domain), it was detected that the achievements of the semi-active suspension improved those of a passive one. To increase the validity of the study, the herein obtained results were compared with other reported studies.

The remainder of this article is structured as follows: Section 2 describes the dynamics and formulation of the one-quarter semi-active suspension model that includes the actuator (MR damper). Section 3 describes the ARX predictive control strategy, the mathematical formulation of the driver block, and the predictive model. Section 4 describes the performance criteria that needs to be fulfilled during the simulation. Section 5 shows the experimental example and results of the semi-active suspension in close loop with the predictive controller. Section 6 reports summarized conclusion and future work.

2. One-Quarter Semi-Active Suspension, Including the Actuator's Dynamics

This section explains the nonlinear model that interacts with the actuator and controller. The semi-active suspension includes the actuator's dynamics such as hysteresis, saturation and the flow of a rheological fluid with micron-sized iron particles through channels that connect two chambers of the magneto-rheological damper. It is worth mentioning that this research considers the actuator's physical limitations in all the carried out work.

The suspension model applied in this work is the one reported in [17]. The authors explain the dynamics of the one-quarter 2-DOF passive suspension, as well as the process of replacing the passive damper with an MR damper modeled via a modified Bouc-Wen approach. Furthermore, the paper explains how to simplify the damper's model to work

just with the Bouc-Wen representation, and this description is the one applied herein. Figure 1 illustrates the semi-active suspension and its elements, elements, where m_s stands for sprung mass, m_{us} represents the unsprung mass, k_s symbolizes the suspension spring, and k_t represents the tire stiffness. Moreover, z_s represents the sprung mass displacement, z_{us} stands for unsprung mass displacement, and z_p symbolizes the road profile.

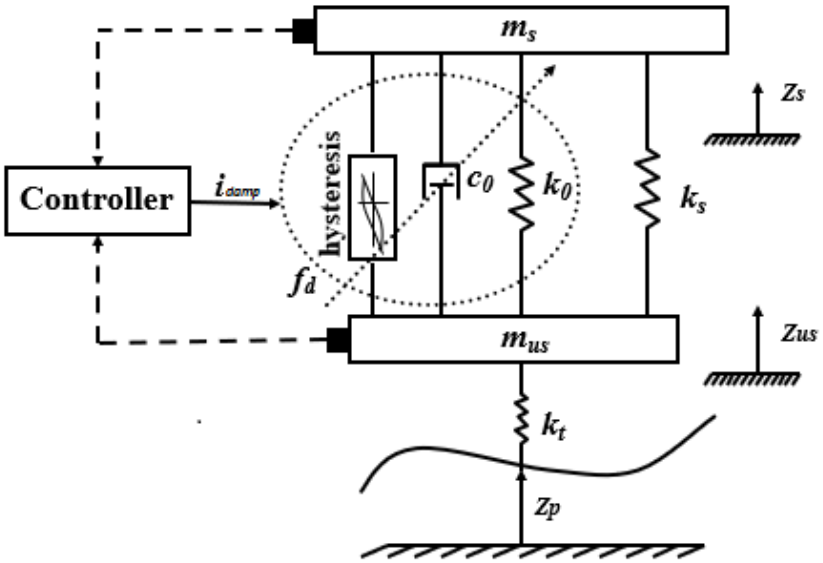

Figure 1. Semi-active One-quarter-vehicle suspension model with a magneto-rheological (MR) damper. The actuator is represented by means of the Bouc-Wen model. Figure taken and modified from [46].

In Figure 1 the element controller represents a general approach, where it reads data from the system (through sensors), applies a control law, and generates a controller's output to modify the force f_d and considering the theoretical variable z_{BW} as well as the internal actuator´s dynamics and transient time behavior, the following equations are obtained:

$$m_s\ddot{z}_s = -c_0(\dot{z}_s - \dot{z}_{us}) - (k_0 + k_s)(z_s - z_{us}) - \alpha z_{BW} \tag{1}$$

$$m_{us}\ddot{z}_u s = -c_0(\dot{z}_{us} - \dot{z}_s) - (k_0 + k_s)(z_{us} - z_s) - k_t(z_{us} - z_p) + \alpha z_{BW} \tag{2}$$

$$\dot{z}_{BW} = -\gamma|\dot{z}_s - \dot{z}_{us}|z_{BW}|z_{BW}|^{n-1} - \beta(\dot{z}_s - \dot{z}_{us})|z_{BW}|^n + \delta(\dot{z}_s - \dot{z}_{us}) \tag{3}$$

where k_0 represents large velocities stiffness, c_0 stands for viscous damping, and α is a coefficient related to the hysteresis behavior; moreover, z_{BW} is a theoretical displacement employed to mathematically model the hysteresis phenomenon exhibited in magneto-rheological dampers [12]. In Equation (3), $n = 2$ where n is defined based on the hysteresis shape, and it is an even quantity for hard hysteresis loops, whereas an uneven quantity of n is employed when the hysteresis curve is smooth. Coefficients β, γ and δ define the hysteresis shape, i.e., how stretched/compressed the hysteresis curve in terms of the relation relative velocity vs force. For more information about the internal variable z_{BW} the hysteresis shape and its coefficients, as well as the coefficients in Equation (3), refer to [12]. Due to the MR damper's dynamics, c_0, k_0, and α are defined as follows:

$$k_0 = k_{0a} + k_{0b}i_{damp} \tag{4}$$

$$c_0 = c_{0a} + c_{0b} i_{damp} \tag{5}$$

$$\alpha = \alpha_a + \alpha_b i_{damp} \tag{6}$$

In Equations (4) to (6), i_{damp} represents the applied current to the MR damper. As explained in [47], c_0, k_0, and α are defined fourth and fifth order polynomials as functions of i_{damp}. However, during the work in [17] it was observed that if the current is kept within [0.2–1.75] A, the behavior of c_0, k_0, and α could be approximated to first order polynomials, then k_{0a}, c_{0a}, and α_a are the base value of k_0, c_0, and α, respectively, when i_{damp} is equal to 0.2 A. Moreover, k_{0b}, c_{0b}, and α_b are additional values for k_0, c_0, and α, respectively, but proportional to i_{damp} when current is greater than 0.2A. To avoid adding complexity to the model, this consideration is applied herein and Equations (4) to (6) hold.

There is another actuator's dynamic that should be considered in the modeling. When a current is applied to the MR damper's terminals, electromagnetic fields are generated and they affect the rheological fluid with micro-iron particles flowing inside the damper. This phenomenon causes the actuator's internal fluid to change from viscous to semisolid in less than 10 milliseconds [8]; so it is required to include this transient dynamics and it can be modeled as a first order differential equation. In Equation (7), i_{damp} symbolizes the current applied to the damper, time constant is equal to 1/140 s, whereas u is the current that impacts on Equations (4) to (6). Observe that Equation (7) is a first order system with a response speed defined by the time constant. This phenomenon was observed and reported in [8].

$$\dot{u} + 140u = 140 i_{damp} \tag{7}$$

Equation (7) represents another actuator's physical limitation, and including it in the system modeling, contributes to generate results that consider more physical aspects of the vehicle suspension. With the model explained, the next step is to design the controller.

3. Predictive Control Based on an ARX Model

The proposed control strategy for the one-quarter semi-active vehicle suspension is shown in Figure 2. The predictive controller is made up by the driver block and the predictive model block. In this control strategy a driving desired trajectory is generated by the driver block using the output of a stable model with a desired dynamics, having the set point as input and the actual process outputs as initial conditions [48]. Within the predictive part of the scheme, the predictive model calculates the control signal from the desired output generated by the driver block that renders, according to the predictive control principle, the desired output equal to the system predicted output.

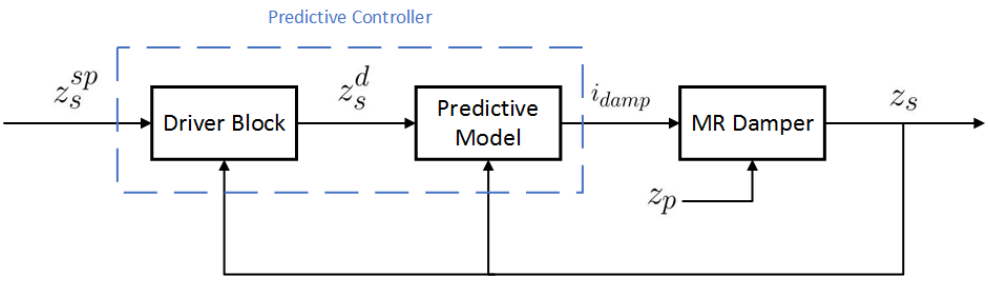

Figure 2. Predictive control strategy for a one-quarter semi-active vehicle suspension.

3.1. Driver Block

The driver block (DB) guides the desired output path to the setpoint commonly using a first order model or a critically damped second order model. Thus, the system's output tends towards the setpoint following a desired trajectory. This trajectory is produced and

redefined at every control instant by the driver block that guides the process output to the desired setpoint as described in [49].

The desired output $z_s^d(k+\lambda|k)$ that is computed at time k by the driver block is obtained using Equation (8).

$$z_s^d(k+\lambda \mid k) = \sum_{i=1}^{p} \varphi_i{}^{(\lambda)} z_s(k+1-i) + \sum_{i=2}^{q} \delta_i{}^{(\lambda)} z_s^{sp}(k+1-i) + \mu^{(\lambda)} z_s^{sp}(k) \tag{8}$$

where, p and q represent the number of the autoregressive terms and the exogenous variable coefficients, respectively, of the driver block model. The prediction horizon λ represents the number of future control intervals set to predict the process output $z_s(k)$. The φ, δ, and μ are the desired trajectory model coefficients projected over λ, and are calculated through the recursive evaluation of Equations (9)–(11).

$$\varphi_i{}^{(j)} = \varphi_1{}^{(j-1)} \alpha_i + \varphi_{i+1}{}^{(j-1)}. \qquad \begin{matrix} i = 1, \ldots, p. \\ j = 2, \ldots, \lambda. \end{matrix} \tag{9}$$

$$\delta_i{}^{(j)} = \varphi_1{}^{(j-1)} \beta_i + \delta_{i+1}{}^{(j-1)}. \qquad \begin{matrix} i = 1, \ldots, q. \\ j = 2, \ldots, \lambda. \end{matrix} \tag{10}$$

$$\mu^{(\lambda)} = \delta_1{}^{(\lambda)} + \delta_1{}^{(\lambda-1)} + \cdots + \delta_1{}^{(1)}. \tag{11}$$

under the initial conditions $\varphi_i{}^{(1)} = \alpha_i$ for $i = 1, \ldots, p$, $\delta_i{}^{(1)} = \beta_i$ for $i = 1, \ldots, q$, $\varphi_{p+1}{}^{(j-1)} = 0$ and $\delta_{q+1}{}^{(j-1)} = 0$ for $j = 2, \ldots, \lambda$, as described in [48].

3.2. Predictive Model

The performance of the control system depends not only on the applied control strategy, but also upon a mathematical model that considers such interaction between all variables in the system as formulated in Equation (12). The model coefficients $\hat{a}_i$ and $\hat{b}_i$ must be obtained looking for the parameters values that best fits the system dynamics.

$$z_s(k) = \sum_{i=1}^{\hat{n}} \hat{a}_i z_s(k-i) + \sum_{i=1}^{\hat{m}} \hat{b}_i i_{damp}(k-i). \tag{12}$$

where $\hat{n}$ represents the order of the AR model and $\hat{m}$ represents the order of the exogenous input, $z_s(k)$ and $i_{damp}(k)$ are the system output and control input respectively.

The control signal $i_{damp}(k)$ for the entire prediction horizon λ is calculated as follows:

$$i_{damp}(k) = \frac{1}{\hat{h}^{(\lambda)}} \left[z_s^{sp}(k+\lambda \mid k) - \sum_{i=1}^{\hat{n}} \hat{e}_i^{(\lambda)} z_s(k+1-i) - \sum_{i=2}^{\hat{m}} \hat{g}_i^{(\lambda)} i_{damp}(k+1-i) \right] \tag{13}$$

In Equation (13), $\hat{e}$ and $\hat{g}$ represents the coefficients of the predictive model projected over prediction horizon λ. Coefficients $\hat{e}$, $\hat{g}$ and $\hat{h}$ are estimated using Equations (14)–(16).

$$\hat{e}_i^{(j)} = \hat{e}_1^{(j-1)} \hat{a}_i + \hat{e}_{i+1}^{(j-1)}. \qquad \begin{matrix} i = 1, \ldots, \hat{n}. \\ j = 2, \ldots, \lambda. \end{matrix} \tag{14}$$

$$\hat{g}_i^{(j)} = \hat{e}_1^{(j-1)} \hat{b}_i + \hat{g}_{i+1}^{(j-1)}. \qquad \begin{matrix} i = 1, \ldots, \hat{m}. \\ j = 2, \ldots, \lambda. \end{matrix} \tag{15}$$

$$\hat{h}^{(\lambda)} = \hat{g}_1^{(\lambda)} + \hat{g}_1^{(\lambda-1)} + \cdots + \hat{g}_1^{(1)}. \tag{16}$$

under the initial conditions $\hat{e}_i^{(1)} = \hat{a}_i$ for $i = 1, \ldots, \hat{n}$, $\hat{g}_i^{(1)} = \hat{b}_i$ for $i = 1, \ldots, \hat{m}$, $\hat{e}_{\hat{n}+1}^{(j-1)} = 0$ and $\hat{g}_{\hat{m}+1}^{(j-1)} = 0$ for $j = 2, \ldots, \lambda$. Detailed analysis of these equations can be found in [49]

In general the proposed predictive controller can be summarized in Table 1.

Table 1. Predictive control algorithm.

Step	Description
1	Get reference $z_s^{sp}(k)$
2	Get process output $z_s(k)$
3	Compute $\varphi_i{}^{(\lambda)}$, $\delta_i{}^{(\lambda)}$, $\mu^{(\lambda)}$
4	Compute $z_s^d(k+\lambda \mid k)$
5	Compute $\hat{e}_i^{(\lambda)}$, $\hat{g}_i^{(\lambda)}$, $\hat{h}^{(\lambda)}$
6	Compute control signal $i_{damp}(k)$

4. Performance Criteria

This endeavor refers to specific quantitative and qualitative performance criteria defined in frequency and time domains.

In this investigation, passenger comfort is related to vibrations coming to the road profile. The vehicle is exposed to a range of vibrations from this source, which travel through the physical elements of the automobile and are transmitted to passengers. These oscillations cause an uncomfortable sensation when they are within a particular range of frequencies and exceed certain amplitude values, i.e., motion sickness is stronger around 1 Hz and 4 Hz, depending on the body resonant frequencies [50]. Although passenger comfort level is very subjective, it is necessary to apply a standard to qualify this criterion.

Vehicle stability depends on the automobile reaction to steering wheel changes, and disturbances from the environment, such as wind currents and road profile irregularities [2]. Therefore, the stability herein focuses on a vehicle's ability to keep the tires in contact with an uneven road profile. The indexes are based on a typical compact city vehicle as reported in [2,51,52].

- *Passenger comfort in low frequencies*.
  Below 5 Hz, keep the relation gain between the sprung mass displacement and the road profile, i.e., (z_s/z_p) less than 2. The aim is to decrease the maximum peak (around 1 Hz for an average city vehicle). For this criterion, z_p is a sinusoidal signal defined by $z_p = 0.015sin(wt)$ m.
- *Vehicle stability between 0 and 15 Hz*.
  Measured through the division of the relation (z_{us}/z_p), i.e., unsprung mass displacement over the road profile. The goal is to cut down the maximum peak observed in the range [10–13] Hz, for an average city vehicle. For this test, z_p is represented by $0.001sin(wt)$ m.
- *Passenger Comfort; the acceleration criterion*.
  From 4 to 30 Hz, keep the root mean square acceleration (rms) of the sprung mass (one quarter of the chassis), below the maximum rms vertical acceleration limit developed by the International Standard ISO 2631 as explained in [2], to assure passenger comfort for up to 8 h. To run this test, apply the z_p as in vehicle stability.
- *Suspension Deflection*.
  From 0 to 4 Hz, keep $(z_s - z_{us})$ within the physical limits of shock absorber to avoid unmodeled dynamics and a premature suspension wear-off. The herein employed MR damper has $\pm$2.5 cm as displacement physical limits, as explained in [47]. For this test, z_p is the same defined for passenger comfort in low frequencies.
- *Performance in time domain*.
  With z_p representing a road bump profile; the objective is to decrease, as much as possible, overshoot, undershoot and settling time for: (z_s/z_p), (z_{us}/z_p), rms of z_{us}, and $(z_s - z_{us})$. The degree of improvement is measured with respect to passive suspension.

In this section, the suspension performance criteria were described. These indexes are widely applied in the literature to determine if passenger comfort and vehicle stability

conditions are satisfied. In this context, they are applied herein as the instrument to evaluate the closed-loop system's performance.

5. Results and Discussion

This section is dedicated to explain the case study where the predictive controller was applied. It includes all the simulation work and testing scenarios as well as the obtained results.

5.1. Simulation Work

To support the theoretical contribution, simulation work was carried out in MATLAB-Simulink with numerical data from a real MR damper characterized in [53] and applied in [21]. The numerical values related to the theoretical variable z_{BW} depicted in Equation (3) are: $\gamma = 1.2e^5$ m^{-2}, $\beta = 1.0e^5$ m^{-2} and $\delta = 15$ and come from the aforementioned vehicle oriented MR damper's characterization reported in [47].

Moreover, the numerical values of: c_{0a}, c_{0b}, k_{0a}, k_{0b}, α_a, and α_b in Equations (4) to (6) are defined in Equations (17) to (19). As mentioned before, it is observed that the total values of: c_0, k_0 and α depend on the current i_{damp}. For this case study, the current feeding the actuator is restricted with the range [0.2–1.75] A to keep Equations (4) to (6) as first order polynomials as explained in [18].

$$k_0 = 604.11 - 256.75 * i_{damp}(\text{N/m}) \tag{17}$$

$$c_0 = 516.63 + 144.883 * i_{damp}(\text{N/m}) \tag{18}$$

$$\alpha = 53290 + 29013 * i_{damp}(\text{N/m}) \tag{19}$$

In Table 2, the numerical values of: m_s, m_{us}, k_s, and k_t were chosen to be within real ranges for one-quarter vehicle suspensions, as applied in [21]. Besides, the results of the semi-active suspension that with the proposed predictive controller will be compared against the performance of a passive suspension that commonly uses a constant $c = 1000$ Ns/m.

Table 2. One-quarter semi-active vehicle suspension parameters.

Parameter	Value
m_s	450 kg
m_{us}	45 kg
k_s	16,000 N/m
k_t	210,000 N/m
c	1000 Ns/m

To include the actuator's physical limitation related to achieve rheologic equilibrium due to a change in the manipulation signal i_{damp}, the transient time to reach the new steady state follows a the well known first order response as explained in Section 2, and its time constant is equal to 0.00714 s, which also comes from a real MR damper's characterization [53]. Equation (7) models the transient actuator's response.

5.2. Predictive Controller Design

For the identification that defines the predictive model parameters $\hat{a}_1$, $\hat{a}_2$, $\hat{b}_1$ and $\hat{b}_2$, the chassis displacement z_s was used as a system's output and the electrical current as a control signal for the MR damper limited from 0.2 to 1.75 A.

As explained in Section 3 the predictive control is built by two parts, the driver block and the predictive model. For the semi-active suspension a first order model was used in the driver block and an identification process using recursive least squares was carried out to estimate the predictive model parameters.

Equation (20) shows the recursive equation for the driver block.

For the driver block a first order model is used and shown in Equation (20),

$$z_s^d(k+\lambda \mid k) = \varphi_1{}^{(\lambda)} z_s(k) + \delta_2{}^{(\lambda)} z_s^{sp}(k-1) + \mu^{(\lambda)} z_s^{sp}(k) \tag{20}$$

where φ_1, δ_2 and μ were obtained from Equations (9)–(11), $\alpha_1 = 0.995$ and $\beta_1 = 0.000995$ were set experimentally.

The Equation (21) was used as the recursive equation for the predictive model. From the experimental work, $\lambda = 2$ was chosen, and sampling time $T_s = 1$ ms were selected based on the vehicle semi-active suspension transient time response.

$$z_s(k) = \sum_{i=1}^{2} \hat{a}_i z_s(k-i) + \sum_{i=1}^{2} \hat{b}_i i_{damp}(k-i). \tag{21}$$

where $\hat{a}_1 = -0.000352$, $\hat{a}_2 = 0.000221$, $\hat{b}_1 = 0.0295$, $\hat{b}_2 = -0.0286$.

Due to the symmetry behavior of the MR damper, the control signal in this case must be the absolute value of Equation (13) and is redefined as:

$$|i_{damp}(k)| = \frac{1}{\hat{h}^{(\lambda)}} \left[z_s^{sp}(k+\lambda \mid k) - \sum_{i=1}^{2} \hat{e}_i^{(\lambda)} z_s(k+1-i) - \hat{g}_i^{(\lambda)} i_{damp}(k+1-i) \right] \tag{22}$$

5.3. Results in the Frequency Domain

The performance of the semi-active predictive and passive suspensions is shown and compared in frequency domain in Figures 3–6, the simulation was carried out under the same simulation conditions for both cases. Each graph is analyzed according to the comfort criteria defined in Section 4 and results are summarized in following subsections.

The ride comfort performance is shown in Figure 3, where it is observed that the predictive controller keeps the z_s/z_p gain under 2 in the maximum peak, whereas the passive suspension fails with a gain above 3. In this case, the predictive suspension complies with the allowed z_s/z_p maximum gain described in the ride comfort criteria. It is also observed that the gain begins to increase at a slower rate than in the passive case, and the maximum gain shifts a little to a higher frequency.

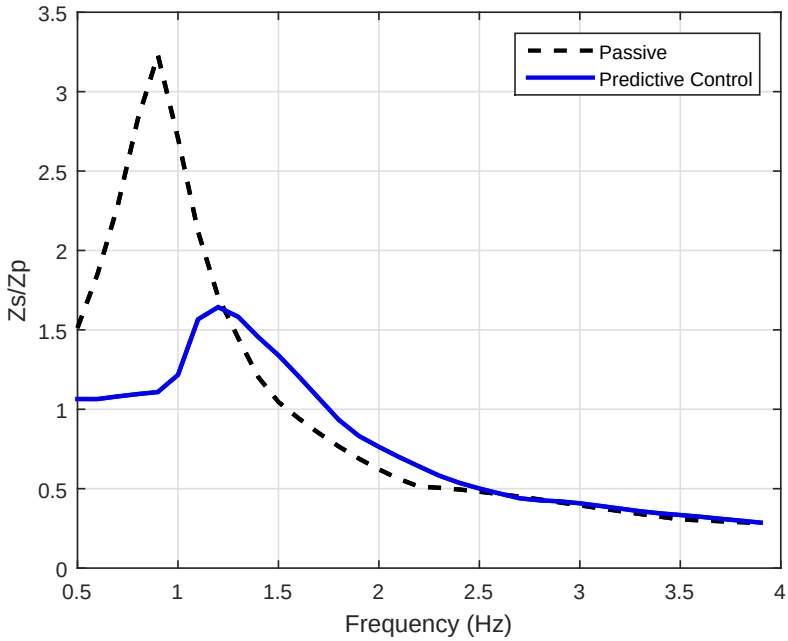

Figure 3. Sprung displacement gain (z_s/z_p) for the passive and predictive controller.

Figure 4 shows the performance in terms of road holding, where the predictive suspension keeps the gain z_u/z_p below 2 and shifts the tire displacement peak to low frequencies. A notable reduction of the the resonant peak (around 11 Hz) over the passive suspension can be seen, where the maximum gain measured for the predictive controller is below 1 around the resonant peak. By keeping the gain less than 2, a road holding is ensured around the resonant frequency, and throughout the analyzed frequency range.

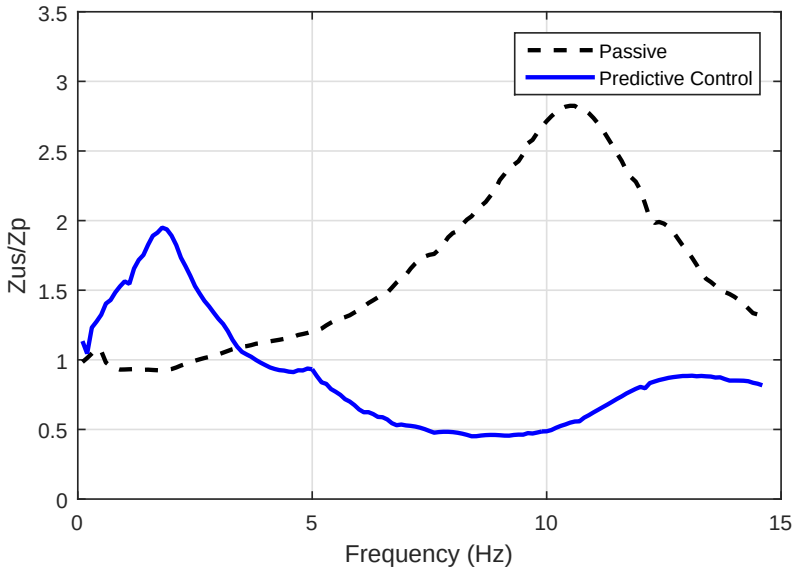

Figure 4. Unsprung mass displacement gain (z_{us}/z_p) for the passive and predictive controller.

In Figure 5, it is shown that the chassis acceleration of the proposed predictive controller maintains the acceleration constant during all frequencies. Moreover, it does not have the peak, around 11 Hz exhibited by the passive suspension. Over the entire frequency range, the chassis acceleration of the semi-active suspension is below the comfort criterion at high frequencies. The outcome in Figure 5 shows a semi-active suspension (with a predictive controller) able to guarantee passenger comfort for eight hours. Although the passive approach keeps the rms acceleration of the passenger at a lower value than the semi-active one, the important fact is that the semi-active suspension also meets this comfort criterion.

Suspension travel performance is shown in Figure 6. In this case the passive suspension reaches out the maximum travel limit ($\pm$2.5 cm), whereas the semi-active predictive suspension has a maximum value equal to 1.63 cm at around 1.4 Hz. This result means that only the predictive suspension is able to comply with the suspension travel criterion. Furthermore, the semi-active suspension would not have the problem of excessive wear-off of the passive suspension. It must be remembered that reaching the physical limits implies forcing the shock absorber, and being in an working zone with not modeled dynamics.

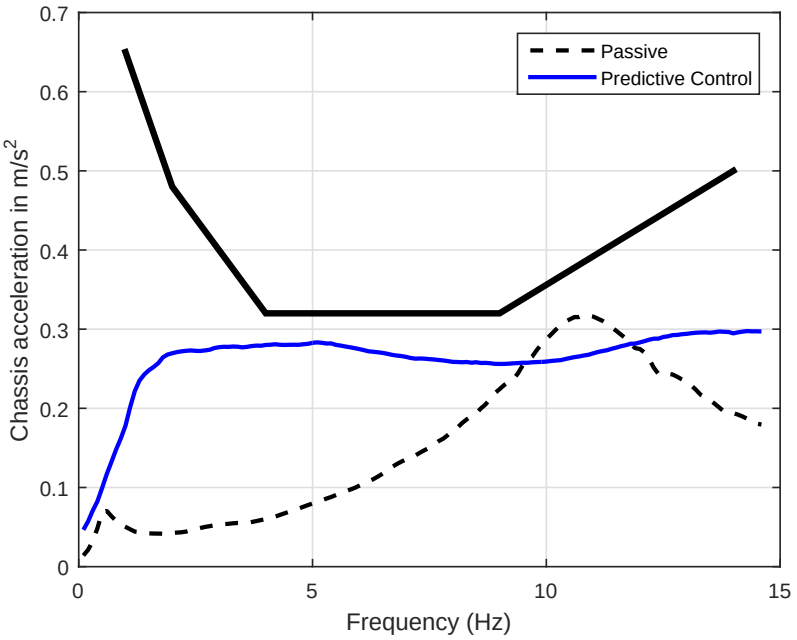

Figure 5. Chassis acceleration relation $\ddot{z}_s$ for the passive and predictive controller. Black line indicates the limit of the acceleration comfort.

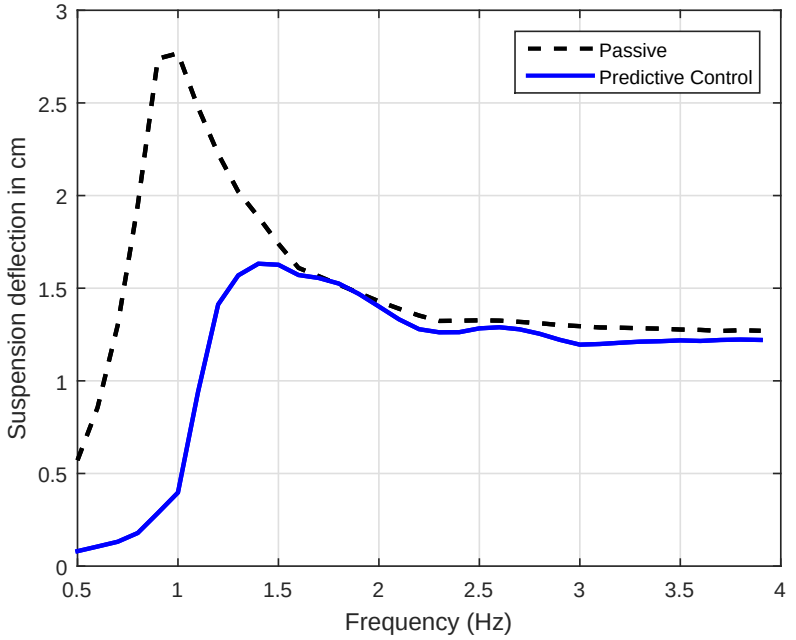

Figure 6. Suspension deflection ($z_s - z_{us}$) for the passive and predictive controlled suspensions.

5.4. Results in Time Domain

This test refers to the suspension response when z_p is a road bump like signal. The goal is to reduce, as much as possible, the overshoot and settling time of z_s, z_{us}, ($z_s - z_{us}$), and $\ddot{z}_s$ with respect to the passive suspension.

Even thought when there are not quantitative performance indexes for time domain analysis, in Figure 7 is possible to identify an improvement in the chassis displacement z_s. The semi-active damper reduces the chassis displacement 26% compared with the passive damper during the bump disturbance and is able to absorb 92% of the damping harmonic motion once the car is out of the bump. Moreover, in the semi-active system the chassis

movement converges faster to the equilibrium position than the passive case; thus, the chassis to oscillate less and this provides a better passenger's comfort feeling. In Figure 8 is observed that the displacement of the tire is almost the same as the road profile, so it manages to slightly improve the performance of the passive suspension. As consequence, the tire maintains the contact with the road profile, thus, keeping the road holding.

With respect to passenger comfort, the chassis acceleration $\ddot{z}_s$ in Figure 9 shows a poor performance in compare with the passive suspension. In the semi-active suspension the maximum acceleration peaks during the bump decreased; however, both the frequency and steady-state time are larger than the passive suspension. This performance is an opportunity area of the semi-active system that could be the subject of a further research study. The suspension deflection ($z_s - z_{us}$) in Figure 10 was also considerably improved, the maximum deflection of the semi-active suspension was 0.07 cm, whereas the passive suspension reached 1.26 cm. Furthermore, this is one of the most outstanding results in the time domain test due to the degree of improvement with respect to the passive suspension. The suspension travel is kept small and this helps isolate passengers from road disturbances.

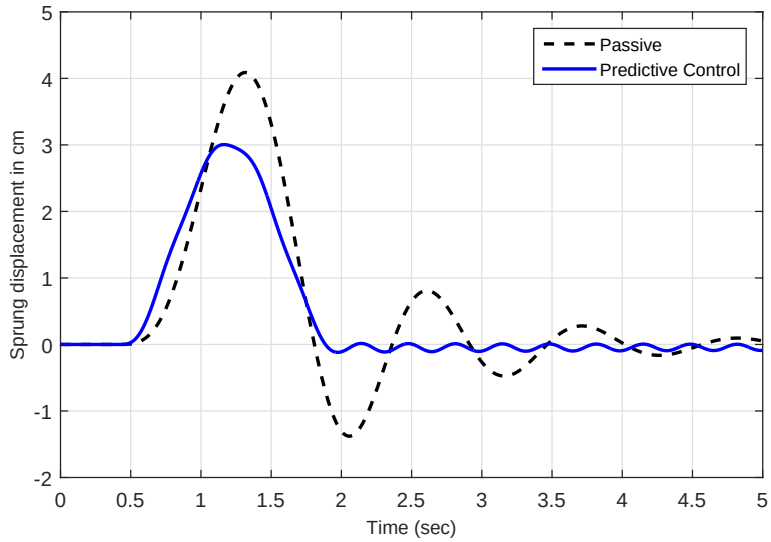

Figure 7. Chassis or sprung mass displacement for the predictive controlled and passive suspensions.

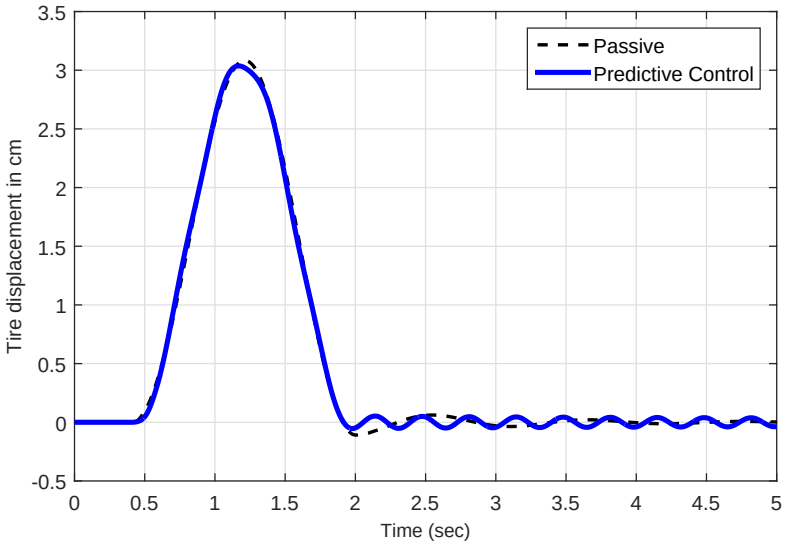

Figure 8. Tire or unsprung mass displacement for the predictive controlled and passive suspensions.

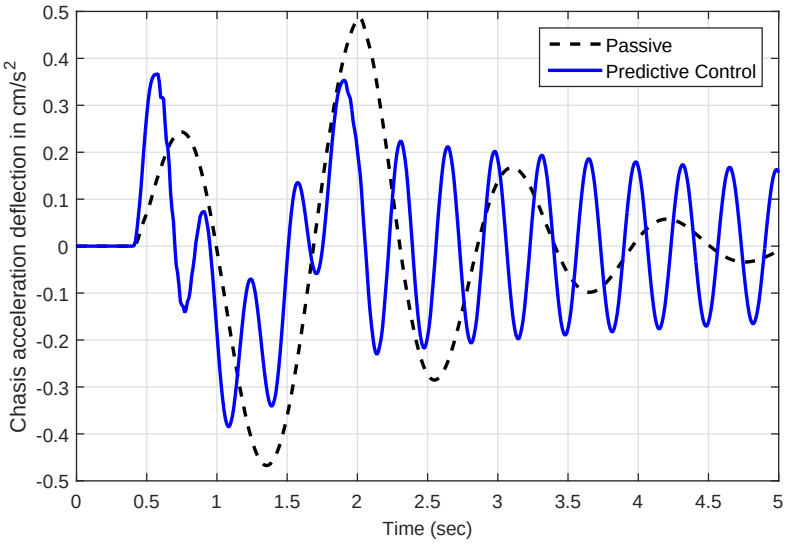

Figure 9. Chassis acceleration for the predictive controlled and passive suspension.

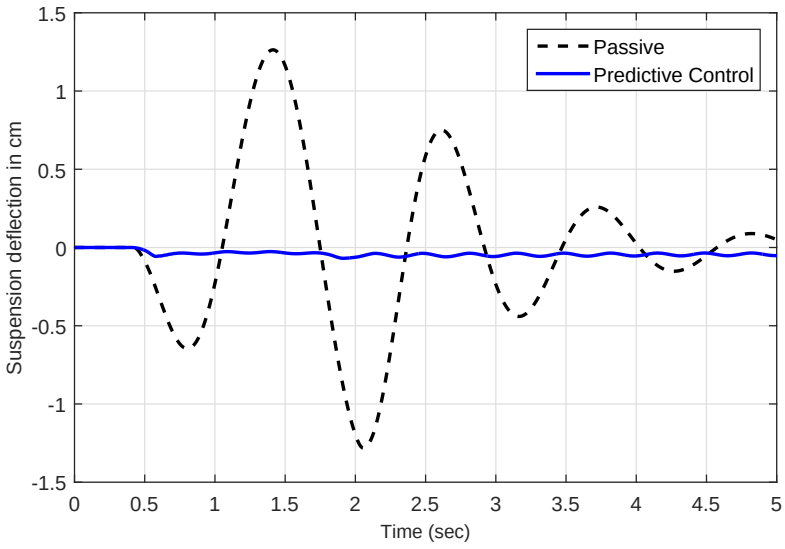

Figure 10. Suspension deflection for the predictive controlled and passive suspensions.

The herein reported results in frequency and time domains significantly improve the passive suspension performance.

The quantitative results of the semi-active predictive suspension satisfied the five performance criteria described in Section 4. In terms of performance, the predictive controller not only significantly improves passive suspension performance and complies with all stated comfort and stability specifications, but also improves the performance of the semi-active over another strategies reported in the literature (see Tables 3 and 4).

Remarkable improvements are observed in the semi-active predictive suspension over the passive suspension. For example a 49.2% reduction of the (z_s/z_p) gain is achieved, 34% reduction in the (z_{us}/z_p) gain was obtained and 41% reduction in the suspension deflection was attained. All these improvements are focused on a considerable peak reduction with respect to the passive suspension.

Table 3. Summary of frequency response results.

Suspension	(z_s/z_p) Gain	(z_{us}/z_p) Gain	$\ddot{z}_s$	Max $(z_s - z_{us})$ in cm.
Passive	3.23	2.97	✓	2.77 ×
Semi-active Predictive	1.64	1.95	✓	1.63 ✓

✓ Meets comfort requirements; × Requirements not met

To have a broader picture of the herein achieved outcomes, a comparison versus another reported results is included. Table 4 shows percentages of improvement of four reported endeavors and the proposed predictive controller. Despite, they employ different one-quarter vehicle parameters, and not all performance indexes are measured with the same method, the percentage of achieved improvement with respect to the reported passive suspension is reported to compare all control strategies. The quantities are the percentage of improvement when maximum values are measured for each category. To calculate the percentages of improvement, measurements were carried out on the reported graphs, for each performance index. In Table 4 the predictive control shows a remarkable improvement regarding to chassis displacement (z_s/z_p) and unsprung mass displacement (z_{us}/z_p) over the H_∞ reported in [18]. Moreover the suspension deflection $(z_s - z_{us})$ maximum value achieved with the predictive controller improved the performance when compared against the results of the LPV/H_∞ reported in [51], but not enhanced the performance of H_∞. The rms chassis acceleration $\ddot{z}_s$ enhanced the results reported in [18,21] in 12% around 11 Hz (value close to the resonance frequency).

Table 4. Percentage of improvement of reported work and proposed predictive control strategy against passive case. Result are reported in frequency domain.

	LPV/H_∞ [51]	LPV/H_∞ [52]	H_∞ [18]	H_2 [21]	Predictive Control
(z_s/z_p)	Not Reported	12.1	46	40.8	49.2
(z_{us}/z_p)	8	7	39.7	40	68.9
$(z_s - z_{us})$	16.2	8	65	61	41
$\ddot{z}_s$	18	25.4	Negative	Negative	14

6. Conclusions and Future Work

The predictive control based on an ARX model, which was applied to the semi-active suspension with an MR damper, improves the performance of the passive suspension and meets all performance criteria. The proposed predictive control improves: 49.2% the sprung displacement gain (z_s/z_p), 68.9% the unsprung displacement gain, 41% the suspension deflection (z_{us}/z_p) and 14% the rms chassis acceleration. Furthermore, when the results are compared with another reported efforts with similar performance criteria in the frequency domain, it is observed that the herein proposed predictive controller competes and improves most of the declared criteria. This finding remarks the contribution of the proposed predictive control strategy based on an ARX model when applied to improve comfort and stability in suspensions of ground vehicles.

Having included the non-linear dynamics of the actuator is very valuable because the simulated scenarios contribute to a closer representation of reality, and the findings become more relevant for the suspension performance evaluation and further decision making.

In general, the proposed semi-active predictive suspension shows a really good performance in terms of computational effort running in a parallel 1-ms sampling time, even when this controller is modeled in a recursive manner. This fact motivates us to look for an option for its implementation in the field with the embedded controller, not only for automotive suspensions, but also in the field of industrial shock absorbers and industrial dampers for solar tracking.

Future work is intended to improve the chassis acceleration response by reducing the oscillation amplitude shown in Figure 9; however, a new identification effort needs to be

performed to adjust the predictive model. Another improvement could be to include the $\ddot{z}_s$ as part of the predictive model to reduce chassis acceleration. A hybrid predictive strategy could be also explored to consider the complete current range of the MR damper. Another research line could be the adaptive capability of the controller to increase robustness under a mass change or different road profile conditions. Finally, a multi-input multi-output adaptive predictive controller could be introduce as a centralized controller for one-half or full vehicle suspensions.

The findings in a 2-DOF system are limited to the vertical dynamics of one tire and one-quarter of the chassis. Although this simplified version of the vehicle's suspension could reduce the model's accuracy and analysis, it is a widely accepted and employed model to study the vertical dynamics in vehicle suspensions. To increase the impact of the research, a more complete analyses on ride comfort and vehicle stability can be carried out if the study is extended to a one-half vehicle suspension model that also includes the roll or pitch angle dynamics. Moreover, the vertical motions would include half of the vehicle´s suspension and mass. This could be studied in future work

Author Contributions: All Authors A.P., A.F.-C., L.C.F.-H., F.B.-C. and C.L. have contributed as follow: Conceptualization, A.P., A.F.-C. and L.C.F.-H.; methodology, A.P., A.F.-C., L.C.F.-H., F.B.-C. and C.L.; software, A.P. and L.C.F.-H.; validation, A.P.; A.F.-C., L.C.F.-H., F.B.-C. and C.L.; formal analysis, A.P., A.F.-C. and L.C.F.-H.; investigation, A.P., A.F.-C., L.C.F.-H., F.B.-C. and C.L.; writing—original draft preparation, A.P. and L.C.F.-H.; writing—review and editing, A.P., A.F.-C., L.C.F.-H., F.B.-C., C.L.; supervision, A.F.-C., F.B.-C. and C.L.; project administration A.F.-C. All authors have read and agreed to the published version of the manuscript.

Funding: This research received no external funding.

Institutional Review Board Statement: Not applicable.

Informed Consent Statement: Not applicable.

Data Availability Statement: Not applicable.

Acknowledgments: The authors would like to thank Consejo Nacional de Ciencia y Tecnología (CONACyT) and Tecnológico de Monterrey for the financial support for conducting the present research. Thanks also to the Sensors and Devices Research Group, and the Robotics Research Group from the School of Engineering and Sciences of Tecnológico de Monterrey for the support given to develop this work.

Conflicts of Interest: The authors declare no conflict of interest.

Abbreviations

The following abbreviations are used in this manuscript:

ARX	AutoRegressive with eXogenous input
DOF	Degrees of Freedom
LPV	Linear Parameter-Varying control
MPC	Model Predictive Control
MR	Magneto-Rheological

References

1. Milliken, W.; Douglas, M. *Race Car Vehicle Dynamics*; Society of Automotive Engineers, Inc.: Warrendale, PA, USA, 1995.
2. Wong, J.Y. *Theory of Ground Vehicles*, 3rd ed.; John Wiley and Sons, Inc.: New York, NY, USA, 2001.
3. Gillespie, T. *Fundamentals of Vehicle Dynamics*; Society of Automotive Engineers, Inc.: Warrendale, PA, USA, 1992.
4. Goncalves, F. Dynamic Analysis of Semi-Active Control Techniques for Vehicle Applications. Master's Thesis, Virginia Polytechnic Institute and State University, Blacksburg, VA, USA, 2001.
5. Pauwelussen, J.P.; Pacejka, H.B. *Smart Vehicles*; Sweets and Zeitlinger Publishers: Lisse, The Netherlands, 1995.
6. Guglielmino, E.; Sireteanu, T.; Stammers, C.; Ghita, G.; Giuclea, M.M. *Semi-Active Suspension CONTROL, Improved Vehicle Ride and Road Friendliness*; Springer: London, UK, 2008.
7. Butz, T.; Von Stryk, O. Modelling and Simulation of Electro- and Magnetorheological Fluid Dampers. *ZAMM J. Appl. Math. Mech.* **2002**, *82*, 3–20. [CrossRef]

8. Spencer, B.F., Jr.; Dyke, S.; Sain, M.; Carlson, J. Phenomenological Model of a Magnetorheological Damper. *ASCE J. Eng. Mech.* **1997**, *123*, 230–238. [CrossRef]
9. Stanway, R. The development of force actuators using ER and MR fluid technology. In Proceedings of the IEEE Colloquium on Actuator Technology: Current Practice and New Developments, London, UK, 10 May 1996; pp. 6/1–6/5.
10. Carlson, J.D.; Catanzarite, D.M.; St. Clair, K.A. Commercial Magneto-rheological Fluid Devices. *Int. J. Mod. Phys. B* **1996**, *10*, 2857–2865. [CrossRef]
11. Chung, S.; Shin, H.-B. High-Voltage Power Supply for Semi-Active Suspension System with ER-Fluid Damper. *IEEE Trans. Veh. Technol.* **2004**, *53*, 206–211. [CrossRef]
12. Wen, Y.-K. Method for Random Vibration of Hysteretic Systems. *ASCE J. Eng. Mech. Div.* **1976**, *102*, 249–263. [CrossRef]
13. Ambhore, N.; Hivarale, S.; Pangavhane, D.R. A Study of Bouc-Wen Model of Magnetorheological Fluid Damper for Vibration Control. *Int. J. Eng. Res. Technol.* **2013**, *2*, 1–6.
14. Razman, M.A.; Priyandoko, G.; Yusoff, A.R. Bouc-Wen Model Parameter Identification for a MR Fluid Damper Using Particle Swarm Optimization. *Adv. Mater. Res.* **2014**, *903*, 279–284. [CrossRef]
15. Zhu, W.; Rui, X.-T. Semi-active Vibration Control Using a Magnetorheological Damper and a Magnetorheological Elastomer Based on the Bouc-Wen Model. *Shock Vib.* **2014**, *2014*, 1–10.
16. Xie, H.L.; Liu, Z.B.; Yang, J.Y.; Sheng, Z.Q.; Xu, Z.W. Modelling of Magnetorheological Damper for Intelligent Bionic Leg and Simulation of Knee Joint Movement Control. *Int. J. Simul. Model.* **2016**, *15*, 144–156. [CrossRef]
17. Félix-Herrán, L.; Mehdi, D.; Soto, R.; de J Rodríguez-Ortiz, J.; Ramírez-Mendoza, R. Control of a Semi-active Suspension with a Magnetorheological Damper Modelled via Takagi-Sugeno. In Proceedings of the 18th Mediterranean Conference on Control & Automation, Marrakech, Morocco, 23–25 June 2010; pp. 1265–1270.
18. Félix-Herrán, L.C.; Mehdi, D.; de J Rodríguez-Ortiz, J.; Soto, R.; Ramírez-Mendoza, R. *H*∞ control of a suspension with a magnetorheological damper. *Int. J. Control* **2012**, *85*, 1026–1038. [CrossRef]
19. Yang, G.Q.; Zhao, Y.Q. Fuzzy Control of Vehicle Suspension System. *Adv. Mater. Res.* **2012**, *383–390*, 2012–2017. [CrossRef]
20. Kurczyk, S.; Pawelczyk, M. Fuzzy Control for Semi-Active Vehicle Suspension. *J. Low Freq. Noise Vib. Act. Control* **2013**, *32*, 217–226. [CrossRef]
21. Félix-Herrán, L.C.; Mehdi, D.; Ramírez-Mendoza, R.; de J Rodríguez-Ortiz, J.; Soto, R. H_2 control of a one-quarter semi-active ground vehicle suspension. *J. Appl. Res. Technol.* **2016**, *14*, 173–183. [CrossRef]
22. Xue, W.; Li, K.; Chen, Q.; Liu, G. Mixed FTS *H*∞ control of vehicle active suspensions with shock road disturbance. *Veh. Syst. Dyn.* **2018**, *57*, 841–854. [CrossRef]
23. Erol, B.; Oz, M.A.; Ucun, L. Two-degree-of-freedom compensator design for disturbance attenuation problem via higher order sinusoidal input describing functions theory. *Trans. Inst. Meas. Control* **2019**, 1–10. [CrossRef]
24. Wang, G.; Chen, C.; Yu, S. Finite-time sliding mode tracking control for active suspension systems via extended super-twisting observer. *Proc. Inst. Mech. Eng. Part I J. Syst. Control. Eng.* **2017**, *231*, 459–470. [CrossRef]
25. Qin, W.; Shangguan, W.-B.; Yin, Z. Sliding mode control of double-wishbone active suspension systems based on equivalent 2-degree-of-freedom model. *Proc. Inst. Mech. Eng. Part D J. Automob. Eng.* **2020**, *234*, 3164–3179. [CrossRef]
26. De J Lozoya Santos, J.; Tudon-Martinez, J.C.; Ramirez-Mendoza, R.A. LPV Control for a Semi-Active Suspension Quarter of Car-One Parameter Case. In Proceedings of MATEC Web of Conferences 81, Lucerne, Switzerland, 6–10 July 2016; pp. 1–4.
27. Tudón-Martínez, J.C.; Varrier, S.; Morales-Menendez, R.; Sename, O. Fault Tolerant Control in a Semi-Active Automotive Suspension (Control Tolerante a Fallas en una Suspensión Automotriz Semi-Activa) *RIAI Rev. Iberoam. Autom. Inform. Ind.* **2016**, *13*, 56–66. (In Spanish) [CrossRef]
28. Rao, K.D.; Kumar, S. Modeling and Simulation of Quarter Car Semi Active Suspension System Using LQR Controller. In Proceedings of the 3rd International Conference on Frontiers of Intelligent Computing: Theory and Applications (FICTA). Advances in Intelligent Systems and Computing, Bhubaneswar, Odisha, India, 14–15 November 2014; pp. 441–448.
29. Beltran-Carbajal, F.; Valderrabano-Gonzalez, A.; Favela-Contreras, A.; Hernandez-Avila, J.L.; Lopez-Garcia, I.; Tapia-Olvera, R. An Active Vehicle Suspension Control Approach with Electromagnetic and Hydraulic Actuators. *Actuators* **2019**, *8*, 35. [CrossRef]
30. Zapateiro, M.; Pozo, F.; Karimi, H.R.; Luo, N. Semi-active Control Methodologies for Suspension Control With Magnetorheological Dampers. *IEEE/ASME Trans. Mechatronics* **2012**, *17*, 370–380. [CrossRef]
31. Krauze, P.; Kasprzyk, J. Vibration control in quarter-car model with magnetorheological dampers using FxLMS algorithm with preview. In Proceedings of the 2014 European Control Conference (ECC), Strasbourg, France, 24–27 June 2014; pp. 1005–1010.
32. Wu, J.-L. A Simultaneous Mixed LQR /H∞ Control Approach to the Design of Reliable Active Suspension Controllers. *Asian J. Control* **2014**, *19*, 415–427. [CrossRef]
33. Olurotimi A.D.; Jimoh O.P. Neural Network-Based Identification and Approximate Predictive Control of a Servo-Hydraulic Vehicle Suspension System. *Eng. Lett.* **2010**, *18*.
34. Sehr, M.A.; Bitmead, R.R. Stochastic output-feedback model predictive control. *Automatica* **2018**, *94*, 315–323. [CrossRef]
35. Cho, B.K. Active Suspension Controller Design Using MPC with Preview Information. *KSME Int. J.* **1999**, *13*, 168–174. [CrossRef]
36. Çalışkan, K.; Henze, R.; Küçükay, F. Potential of Road Preview for Suspension Control under Transient Road Inputs. *IFAC-PapersOnLine* **2016**, *49*, 117–122. [CrossRef]
37. Shao, S.; Zhou, H.; Liu, H. Distributed Model Predictive Control and Implementation for Vehicle Active Suspensions. I*FAC-PapersOnLine* **2018**, *51*, 961–966. [CrossRef]

38. Hu, Y.; Chen, M.Z.Q.; Hou, Z. Multiplexed model predictive control for active vehicle suspensions. *Int. J. Control* **2014**, *88*, 347–363. [CrossRef]
39. Canale, M.; Milanese, M.; Novara, C. Semi-Active Suspension Control Using "Fast" Model-Predictive Techniques. *IEEE Trans. Control. Syst. Technol.* **2006**, *14*, 1034–1046. [CrossRef]
40. Houzhong, Z.; Jiasheng, L.; Chaochun, Y.; Xiaoqiang, S.; Yingfeng, C. Application of explicit model predictive control to a vehicle semi-active suspension system. *J. Low Freq. Noise, Vib. Act. Control* **2020**, *39*, 772–786. [CrossRef]
41. Giorgetti, N.; Bemporad, A.; Tseng, H.E.; Hrovat, D. Hybrid model predictive control application towards optimal semi-active suspension. *Int. J. Control* **2006**, *79*, 521–533. [CrossRef]
42. Morato, M.M.; Sename, O.; Dugard, L. LPV-MPC Fault Tolerant Control of Automotive Suspension Dampers. *IFAC-PapersOnLine* **2018**, *51*, 31–36. [CrossRef]
43. Guanetti, J.; Borrelli, F. Stochastic MPC for cloud-aided suspension control. In Proceedings of the 2017 IEEE 56th Annual Conference on Decision and Control (CDC), Melbourne, Australia, 12–15 December 2017; pp. 238–243.
44. Wu, J.; Wang, Z.; Zhang, L. Unbiased-estimation-based and computation-efficient adaptive MPC for four-wheel-independently-actuated electric vehicles. *Mech. Mach. Theory* **2020**, *154*, 1–15. [CrossRef]
45. Enders, E.; Burkhard, G.; Munzinger, N. Analysis of the Influence of Suspension Actuator Limitations on Ride Comfort in Passenger Cars Using Model Predictive Control. *Actuators* **2020**, *9*, 77. [CrossRef]
46. Félix-Herrán, L.C.; Soto, R.; de J Rodríguez-Ortiz, J.; Ramirez-Mendoza, R.A. Fuzzy Control for a Semi-Active Vehicle Suspension with a Magnetorheological Damper. In Proceedings of the European Control Conference, Budapest, Hungary, 23–26 August 2009; pp. 4398–4403.
47. Sireteanu, T.; Stancioiu, D.; Stammers, C.W. Modelling of magnetorheological fluid dampers. *Proc. Rom. Acad.* **2001**, *2*, 105–113.
48. Martin-Sanchez, J.M. A new solution to adaptive control. *Proc. IEEE* **1976**, *64*, 1209–1218. [CrossRef]
49. Sánchez, M.; Rodellar, J. *Adaptive Predictive Control: From the Concepts to Plant Optimization*, 6th ed.; Prentice-Hall International Series in Systems and Control Engineering: London, UK, 1996.
50. Bastow, D.; Howard, G.; Whitehead, J. *Car Suspension and Handling*; SAE International: New York, NY, USA, 2004.
51. Poussot-Vassal, C.; Sename, O.; Dugard, L.; Gáspár, P.; Szabó, Z.; Bokor, J. A new semi-active suspension control strategy through LPV technique. *J. Control Eng. Pract.* **2008**, *16*, 1519–1534. [CrossRef]
52. Do, A.; Sename, O.; Dugard, L. An LPV control approach for semi-active suspension control with actuator constraints. In Proceedings of the American Control Conference, Baltimore, MD, USA, 30 June–2 July 2010; pp. 4653–4658. [CrossRef]
53. Lam, H.F.; Lai, C.Y.; Liao, W.H. *Automobile Suspension Systems with MR Fluid Dampers*; Technical Report; Department of Mechanical and Automation Engineering, The Chinese University of Hong Kong: Hong Kong, China, 2002.